Single Atom Transistor in a 1D Optical Lattice

A. Micheli,[1,2] A. J. Daley,[1,2] D. Jaksch,[3] and P. Zoller[1,2]

[1]*Institute for Quantum Optics and Quantum Information of the Austrian Academy of Sciences, A-6020 Innsbruck, Austria*
[2]*Institute for Theoretical Physics, University of Innsbruck, A-6020 Innsbruck, Austria*
[3]*Clarendon Laboratory, University of Oxford, Parks Road, Oxford OX1 3PU, United Kingdom*

(Received 3 June 2004; published 1 October 2004)

We propose a scheme utilizing a quantum interference phenomenon to switch the transport of atoms in a 1D optical lattice through a site containing an impurity atom. The impurity represents a qubit which in one spin state is transparent to the probe atoms, but in the other acts as a single atom mirror. This allows a single-shot quantum nondemolition measurement of the qubit spin.

DOI: 10.1103/PhysRevLett.93.140408 PACS numbers: 03.75.Lm, 03.67.Lx, 42.50.–p

Coupling of a spin 1/2 system to bosonic and fermionic modes is one of the fundamental building blocks of quantum optics and solid state physics. Motivated by the recent progress with cold atoms in 1D [1], we consider a spin 1/2 atomic impurity which is used to switch the transport of either a 1D Bose-Einstein condensate or a 1D degenerate Fermi gas initially situated to one side of the impurity. In one spin state the impurity is transparent to the probe atoms, while in the other it acts as a single atom mirror, prohibiting transport via a quantum interference mechanism reminiscent of electromagnetically induced transparency (EIT) [2] [Fig. 1(a)]. Observation of the atomic current passing the impurity can then be used as a quantum nondemolition (QND) measurement [3] of its internal state, which can be seen to encode a qubit, $|\psi_q\rangle = \alpha|\uparrow\rangle + \beta|\downarrow\rangle$. If a macroscopic number of atoms pass the impurity, then the system will be in a macroscopic superposition, $|\Psi(t)\rangle = \alpha|\uparrow\rangle|\phi_\uparrow(t)\rangle + \beta|\downarrow\rangle|\phi_\downarrow(t)\rangle$, which can form the basis for a single-shot readout of the qubit spin. Here, $|\phi_\sigma(t)\rangle$ denotes the state of the probe atoms after evolution to time t, given that the qubit is in state σ [Fig. 1(a)]. In view of the analogy between state amplification via this type of blocking mechanism and readout with single electron transistors used in solid state systems [4], we refer to this setup as a single atom transistor (SAT).

We propose the implementation of a SAT using cold atoms in 1D optical lattices [5–8]. We consider probe atoms b to be loaded in the lattice to the left of a site containing the impurity atom, which is trapped by a separate (e.g., spin-dependent [8]) potential [Fig. 1(b)]. The passage of b atoms past the impurity q is then governed by the spin-dependent effective collisional interaction $\hat{H}_{\rm int} = \sum_\sigma U_{{\rm eff},\sigma}\hat{b}_0^\dagger\hat{b}_0\hat{q}_\sigma^\dagger\hat{q}_\sigma$. By making use of a quantum interference mechanism, we engineer complete blocking (effectively $U_{\rm eff} \to \infty$) for one spin state and complete transmission ($U_{\rm eff} \to 0$) for the other. Below we first consider the detailed scattering processes involved in the transport of a single particle through the SAT, and then generalize this to interacting many-particle systems including a 1D Tonks gas.

The quantum interference mechanism needed to engineer $U_{\rm eff}$ can be produced using an optical or magnetic Feshbach resonance [9]. For the optical case a Raman laser drives a transition on the impurity site 0 from the atomic state $\hat{b}_0^\dagger\hat{q}_\sigma^\dagger|{\rm vac}\rangle$ via an off-resonant excited molecular state to a bound molecular state back in the lowest electronic manifold $\hat{m}_\sigma^\dagger|{\rm vac}\rangle$ [Fig. 2(a)]. We denote the effective two-photon Rabi frequency and detuning by Ω_σ and Δ_σ, respectively. For the magnetic case, the Hamiltonian will have the same form, but with Ω_σ the coupling between open and closed channels and Δ_σ the magnetic field detuning [9]. The Hamiltonian for our system is then given ($\hbar \equiv 1$) by $\hat{H} = \hat{H}_b + \hat{H}_0$, with

$$\hat{H}_{\rm b} = -J\sum_{\langle ij\rangle}\hat{b}_i^\dagger\hat{b}_j + \frac{1}{2}U_{bb}\sum_j\hat{b}_j^\dagger\hat{b}_j(\hat{b}_j^\dagger\hat{b}_j - 1),$$

$$\hat{H}_0 = \sum_\sigma[\Omega_\sigma(\hat{m}_\sigma^\dagger\hat{q}_\sigma\hat{b}_0 + {\rm H.c.}) + \Delta_\sigma\hat{m}_\sigma^\dagger\hat{m}_\sigma] + \sum_\sigma[U_{qb,\sigma}\hat{b}_0^\dagger\hat{q}_\sigma^\dagger\hat{q}_\sigma\hat{b}_0 + U_{bm,\sigma}\hat{b}_0^\dagger\hat{m}_\sigma^\dagger\hat{m}_\sigma\hat{b}_0], \quad (1)$$

where the operators $\hat{b}$ obey the standard commutation (anticommutation) relations for bosons (fermions). $\hat{H}_b$ gives a Hubbard Hamiltonian for the b atoms with tunneling matrix elements J giving rise to a single Bloch band with dispersion relation $\varepsilon(k) = -2J\cos ka$ (a is the lattice spacing), and collisional interactions (which are nonzero only for bosons) given by $U_{bb} = 4\pi\hbar^2 a_{bb}\int d^3\mathbf{x}|{\rm w}_j(\mathbf{x})|^4/m_b$, where ${\rm w}_j(\mathbf{x})$ is the Wannier function for a particle localized on site j, a_{bb} is the

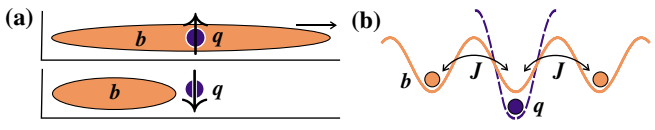

FIG. 1 (color online). (a) A spin 1/2 impurity used as a switch: in one spin state it is transparent to the probe atoms, but in the other it acts as a single atom mirror. (b) Implementation of the SAT as a separately trapped impurity q with probe atoms b in an optical lattice.

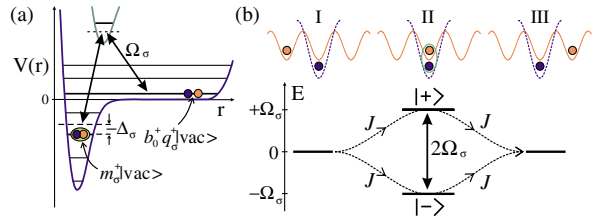

FIG. 2 (color online). (a) The optical Feshbach setup couples the atomic state $\hat{b}_0^\dagger \hat{q}_\sigma^\dagger|\text{vac}\rangle$ (in a particular motional state quantized by the trap) to a molecular bound state of the Born-Oppenheimer potential, $\hat{m}_\sigma^\dagger|\text{vac}\rangle$, with effective Rabi frequency Ω_σ and detuning Δ_σ. (b) A single atom passes the impurity (I $\rightarrow$ III) via the two dressed states (II), $|+\rangle = \hat{b}_0^\dagger \hat{q}_\sigma^\dagger|\text{vac}\rangle + \hat{m}_\sigma^\dagger|\text{vac}\rangle$ and $|-\rangle = \hat{b}_0^\dagger \hat{q}_\sigma^\dagger|\text{vac}\rangle - \hat{m}_\sigma^\dagger|\text{vac}\rangle$ and quantum interference gives rise to an effective tunneling rate $J_{\text{eff},\sigma}$.

scattering length for b atoms and m_b is their mass. $\hat{H}_0$ describes the additional dynamics due to the impurity on site 0, where atoms b and q are converted to a molecular state with effective Rabi frequency Ω_σ and detuning Δ_σ, and the last two terms describe background interactions, $U_{\alpha\beta,\sigma}$ for two particles $\alpha, \beta \in \{q, b, m\}$, which are typically weak. This model is valid for $U_{\alpha\beta}, J, \Omega, \Delta \ll \omega$, where ω is the energy separation between Bloch bands. Because the dynamics for the two spin channels q_σ can be treated independently, in the following we will consider a single spin channel, and drop the subscript σ.

For off-resonant laser driving ($\Omega \ll |\Delta|$), the Feshbach resonance enhances the interaction between b and q atoms, giving the familiar result $U_{\text{eff}} = U_{qb} - \Omega^2/\Delta$. However, for resonant driving ($\Delta = 0$) the physical mechanism changes, and the effective tunneling J_{eff} of an atom b past the impurity [Fig. 2(b), I $\rightarrow$ III] is blocked by quantum interference. On the impurity site, laser driving mixes the states $\hat{b}_0^\dagger \hat{q}^\dagger|\text{vac}\rangle$ and $m^\dagger|\text{vac}\rangle$, forming two dressed states with energies $\varepsilon_\pm = (U_{qb})/2 \pm (U_{qb}^2/4 + \Omega^2)^{1/2}$ [Fig. 2(b), II]. The two resulting paths for a particle of energy ε destructively interfere so that for large $\Omega \gg J$ and $U_{qb} = 0$, $J_{\text{eff}} = -J^2/(\varepsilon + \Omega) - J^2/(\varepsilon - \Omega) \rightarrow 0$. This is analogous to the interference effect underlying EIT [2], and is equivalent to having an effective interaction $U_{\text{eff}} \rightarrow \infty$. In addition, if we choose $\Delta = \Omega^2/U_{qb}$, the paths constructively interfere, screening the background interactions to produce perfect transmission ($U_{\text{eff}} \rightarrow 0$).

For a more detailed analysis, we solve the Lippmann-Schwinger equation exactly for scattering from the impurity of an atom b with incident momentum $k > 0$ in the lowest Bloch band. The resulting forwards and backwards scattering amplitudes, $f^{(\pm)}(k)$ respectively, are

$$f^{(\pm)}(k) = \left[1 + \left(\frac{iaU_{\text{eff}}(k)}{v(k)}\right)^{\pm 1}\right]^{-1}, \qquad (2)$$

where the energy dependent interaction $U_{\text{eff}} = U_{qb} + \Omega^2/[\varepsilon(k) - \Delta]$ and the phase velocity $v(k) = \partial\varepsilon/\partial k = 2Ja\sin ka$. The corresponding transmission probabilities, $T(k) = |f^{(+)}(k)|^2$, are plotted in Fig. 3(a) as a function of $\varepsilon(k)$ for various Ω and Δ. For $\Omega \sim J$, these are Fano profiles with complete reflection at $\varepsilon(k) = \Delta$ and complete transmission at $\varepsilon(k) = \Delta - \Omega^2/U_{qb}$. The SAT thus acts as an energy filter, which is widely tunable via the laser strength and detuning used in the optical Feshbach setup. For $\Omega > 4J$, T is approximately independent of k, and we recover the previous result, i.e., that transport can be completely blocked or permitted by appropriate selection of Δ. Note that this mechanism survives when higher energy Bloch bands are included, and is resistant to loss processes, which are discussed below.

We now consider the full many-body dynamics of N probe atoms b initially prepared in the ground state in a trap (box) of M lattice sites on the left side of the impurity q. We are then interested in the expectation value of the steady state coherent current $\hat{I} = d\hat{N}_R/dt$ [where $\hat{N}_R = \sum_{j>0} \hat{b}_j^\dagger \hat{b}_j$ is the number of particles on the right side of the impurity; see Fig. 3(b)], which depends on the laser parameters, the initial filling factor on the left of the impurity, $n = N/M$, and, for bosons, the interaction strength U_{bb}. We first consider the case of a dilute or noninteracting gas, before treating both interacting bosons and noninteracting fermions with arbitrary n.

For a dilute noninteracting Bose quasicondensate ($n \ll 1$, $U_{bb} = 0$), or for any very dilute gas (where the momentum distribution is very narrow), the behavior is very similar to that of a single particle. If the gas is quickly accelerated to a finite momentum k, e.g., by briefly tilting the lattice, then the atoms will coherently tunnel through the impurity according to the scattering amplitudes $f^{(\pm)}(k)$. The resulting current $I \propto N|f^{(+)}(k)|^2 v(k)$, where $v(k)$ is the velocity of a Bloch wave with momentum k.

For a Fermi gas the equations of motion are linear and may be solved exactly provided $U_{bm} = U_{qb}$. Scattering from the impurity then occurs independently for each particle in the initial Fermi sea, with scattering ampli-

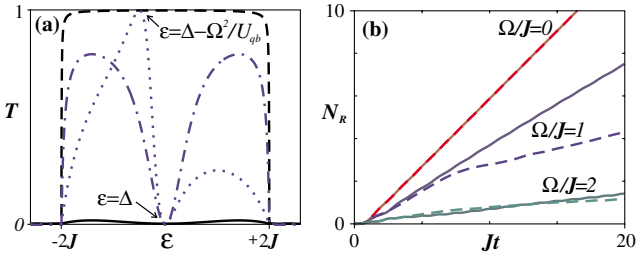

FIG. 3 (color online). (a) SAT transmission coefficients $T \equiv |f^{(+)}|^2$ for a particle b as a function of its energy $\varepsilon(k)$ for $\Omega/J = 4$, $\Delta = 0$, $U_{qb}/J = 0$ (solid line), $\Omega/J = 8$, $\Delta/J = 4$, $U_{qb}/J = 2$ (dashed line), $\Omega/J = 1$, $\Delta = 0$, $U_{qb}/J = 2$ (dotted line), and $\Omega/J = 1$, $\Delta = 0$, $U_{qb}/J = 0$ (dash-dotted line). (b) The number of particles to the right of the impurity, $N_R(t)$, from exact numerical calculations for bosons in the limit $U_{bb}/J \rightarrow \infty$ (dashed lines) and Fermions (solid lines) in a 1D Mott insulator state with $n = 1$, for $\Delta = 0$, $\Omega/J = 0, 1, 2$.

tudes $f^{(\pm)}(k)$ for $k \leq k_F$, where the Fermi momentum $k_F = \pi n/a$. After a short transient period, on the order of the inverse tunneling rate $1/J$, the system establishes a roughly constant flux of particles through the impurity [Fig. 3(b)], with a time-averaged current for resonant driving $\Delta = 0$ given by

$$I_0 = \frac{1}{\pi a}\int_{-2J}^{-2J+\varepsilon_F} d\varepsilon f(\varepsilon)T(\varepsilon)v(\varepsilon) = \frac{J}{\pi}\left[V - \frac{G_+ \arctan\frac{VG_-}{G_+^2 - V} + G_- \operatorname{arctanh}\frac{VG_+}{G_-^2 + V}}{(G_+^2 + G_-^2)/(G_+G_-)}\right], \quad (3)$$

with ε_F the Fermi energy in the initial state, $f(\varepsilon)$ the density of states per site (left of the impurity), $2G_\pm^2 \equiv (1 + \Omega^4/4J^4)^{1/2} \pm 1$ and $V \equiv \varepsilon_F/2J = 2\sin^2(n\pi/2)$.

For a Tonks gas of strongly interacting bosons ($U_{bb}/J \gg 1$ with $n \leq 1$) we expect to observe similar behavior to that observed for fermions. In this limit, double occupation of a site can be neglected, and the behavior can be mapped onto fermionic particles via a Jordan-Wigner transformation (JWT) [10]. The Hamiltonian is then the same up to a nonlinear phase factor $\Omega \to \Omega(-1)^{\hat{N}_R}$, which essentially causes Ω to change sign when a particle passes the impurity. The contribution of this phase factor should be small for weak coupling, $\Omega \ll J$, and also for strong coupling, where no particles will tunnel through the impurity, i.e., $N_R \simeq 0$.

For the general case of many bosons we perform exact numerical integration of the time dependent Schrödinger equation for the Hamiltonian (1) using Vidal's algorithm for "slightly entangled quantum states" [11]. This algorithm selects adaptively a decimated Hilbert space on which a state is represented, by retaining at each time step only those basis states that carry the greatest weight in Schmidt decompositions taken from every possible bipartite splitting of the system into two contiguous parts. A sufficiently large decimated Hilbert space is then selected so that the results of the simulations are essentially exact. For each set of parameters we first prepared the initial state via an imaginary time evolution which found the ground state for atoms in a box trap on the left of the impurity. Then, considering initially a single impurity atom q on the site 0 and unoccupied sites to the right of that site, we calculated the time evolution of the system until it had reached a quasisteady state behavior. In the simulations we obtained the behavior at finite repulsion U_{bb}, and tested the effects of the nonlinear phase factor $(-1)^{\hat{N}_R}$ for strongly interacting bosons, $U_{bb} \to \infty$.

In Fig. 3(b) we plot the number of particles on the right of the impurity $N_R(t)$ for fermions and for bosons with $U_{bb}/J \to \infty$, starting from a Mott insulator (MI) state with $n = 1$, for $\Delta = 0$, $\Omega/J = 0, 1, 2$. For $\Omega = 0$ the results for bosons and fermions are identical, while for $\Omega/J = 1, 2$ we observe an initial period for the bosons in which the current is similar to that for the fermionic systems, after which the bosons settle into a steady state with a significantly smaller current. The initial transient period for the bosons incorporates the settling to steady state of firstly the molecule dynamics, and secondly the momentum distribution on the right of the impurity. These transients are suppressed if Ω is ramped slowly to its final value from a large value $\Omega > 4J$.

The dependence of the steady state current on the initial filling factor n is depicted in Fig. 4(a) for resonant driving with $\Omega/J = 0, 1, 2$. For $\Omega = U_{qb} = U_{bm} = 0$, the current $I_0 = 2J\sin^2(n\pi/2)/\pi$ is identical for fermions and hard-core bosons ($U_{bb} \to \infty$), as we expect from the exact correspondence given in this limit by the JWT. For fermions with weak, resonant laser driving, the main features of the Fano profile [Fig. 3(a)] are observed in correspondence with the integral in (3). For example, a plateau in $I_0(n)$ is observed near $n = \arccos(-\Delta/2J)/\pi = 1/2$, as the Fermi energy is raised past $\varepsilon \sim \Delta = 0$, which corresponds to the zero of the transmission probability $T(\varepsilon)$. Good agreement is also observed with the result for bosons in this limit with $n < 1/2$, while for larger n bosons are blocked better, with a factor of 2 to 3 in the steady state currents.

The enhanced blocking for bosons is also seen in Fig. 4(b) showing the steady state current against Ω for resonant driving and $n = 1$. It is clear from these figures together that this difference is a feature of the regime $n > 1/2$, $\Omega \sim J$, which is directly linked to the phase factor of $(-1)^{N_R}$ arising in the JWT. As Ω is increased and fewer particles pass the impurity, the results for fermions and bosons again converge as expected. For small Ω there are small differences between bosons with finite $U_{bb}/J = 4$ and $U_{bb}/J \to \infty$, with currents always lower than the equivalent fermionic current, owing largely to the smaller mean squared momentum in the initial state. For large driving $\Omega \gg 4J$ the basic interference process is ex-

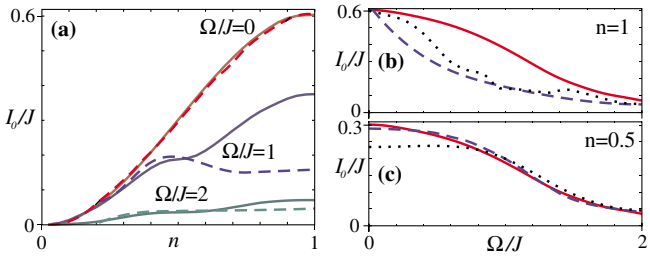

FIG. 4 (color online). (a) The steady state current of b atoms through the impurity as a function of the initial filling factor n for $\Delta = 0$ and $\Omega/J = 0, 1, 2$. The solid lines show the analytic result I_0 for fermions, whereas the dashed lines show the exact numerical result for hard-core bosons with $U_{bb}/J \to \infty$. For $\Omega = 0$ these results are indistinguishable. (b),(c) The steady state current as a function of the Rabi frequency Ω/J on resonance $\Delta = 0$ for (b) unit filling and (c) half filling. The solid lines show the analytic result for fermions, whereas the dashed (dotted) lines give numerical results for bosons with $U_{bb}/J = 20$ ($U_{bb}/J = 4$).

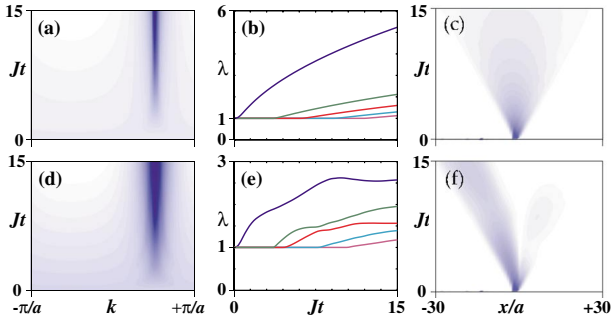

FIG. 5 (color online). Exact numerical results showing the propagation of $N = 30$ hard-core bosons in an initial MI state ($n = 1$) through a SAT with (a)–(c) $\Omega = 0$ and (d)–(f) $\Omega = 0.5J$, with $\Delta = U_{qb} = U_{bm} = 0$. The plot shows (a),(d) the momentum distribution, (b),(e) the five largest eigenvalues λ_m of the single particle density matrix $\langle \hat{b}_i^\dagger \hat{b}_j \rangle$, and (c),(f) the spatial density of the largest eigenmode (the quasicondensate) as a function of time. Darker colors represent higher values.

tremely efficient for bosons and fermions, and we observe complete blocking or transmission by quantum interference for the proper choice of Δ.

In Fig. 5 we investigate the time evolution of 30 hard-core bosons ($U_{bb} \to \infty$) in an initial MI state, which are released through a SAT which is switched at $t = 0$. For $\Omega = 0$, we see that as the gas expands the momentum distribution becomes peaked as a quasicondensate is formed with $k = \pi/2a$, which consists of a coherent superposition of particles propagating to the right and holes propagating to the left as the MI state melts [6]. This mode grows outwards from the edge of the initial distribution, and contains at its peak $\sim\sqrt{N}$ particles, as is expected for such dynamically formed quasicondensates in a 1D lattice [12]. In contrast, for $\Omega/J = 0.5$, the momentum distribution is broader, and the quasicondensate mode contains many fewer particles. The mode also consists of distinct branches, holes in the melting MI propagating to the left and particles to the right, which are initially coherent, but become decoupled at $t \sim 12/J$. For larger Ω this behavior becomes more pronounced, and for $\Omega > 4J$ the MI state essentially remains unchanged.

The melting of a MI in this way can be used as the basis for a convenient single-shot measurement of the spin state of q. If q is in a superposition of spin states, only one of which will permit transport of the b atoms, then after some propagation time the system will be in a macroscopic superposition of distinct quantum phases (MI and quasicondensates). These are distinguishable because if the b atoms are released from the lattice, the quasicondensate will produce an interference pattern, whereas the MI state will not. The visibility of the resulting pattern can thus be used to measure the qubit spin.

A remarkable feature of the SAT is its resistance to both two- and three-body loss processes on the impurity site. Spontaneous emissions from the off-resonant excited molecular state in the case of an optical Feshbach resonance amount to a two-body loss process at a rate $\sim\gamma_{2B}$ in the states $|+\rangle$ and $|-\rangle$. These small rates are further suppressed in the blocking regime $J, \gamma_{2B} \ll \Omega$, with the resulting decoherence rate $\gamma_{\rm dec} \propto J^2\gamma_{2B}n/\Omega^2$, with n the mean site occupation of the b atoms. Collisions of atoms b with molecules m [13] are strongly suppressed in the Tonks gas regime, as well as for fermions. For a weakly interacting Bose gas the corresponding three-body loss rate, γ_{3B}, is again strongly suppressed in the blocking regime ($J, \gamma_{3B} \ll \Omega$) with $\gamma_{\rm dec} \propto J^4\gamma_{3B}n^2/\Omega^4$.

Parallels may be drawn between the SAT and other systems coupled to fermionic and bosonic modes. These include the QND readout of a single photon in cavity-quantum electrodynamics [14], electron counting statistics [15], and the transport of electrons past impurities such as quantum dots [16] (although there particles are normally initially present on both sides of the impurity). However, the long decoherence times for atoms in optical lattices imply coherent transport over longer time scales than is observed in these other systems, which are inherently dissipative. In addition, blocking and/or energy filtering by one or more SATs could be applied as tools in the study of Bose and Fermi gases in a 1D lattice.

Work in Innsbruck is supported by the Austrian Science Foundation, EU Networks, and the Institute for Quantum Information. D. J. is supported by the IRC on quantum information processing.

[1] T. Stöferle *et al.*, Phys. Rev. Lett. **92**, 130403 (2004); B. Paredes *et al.*, Nature (London) **429**, 277 (2004).
[2] M. Lukin, Rev. Mod. Phys. **75**, 457 (2003).
[3] V. B. Braginsky and F. Y. Khalili, *Quantum Measurement* (Cambridge University, Cambridge, England, 1992).
[4] See, for example, G. Johansson *et al.*, cond-mat/0210163.
[5] D. Jaksch *et al.*, Phys. Rev. Lett. **81**, 3108 (1998).
[6] D. Jaksch *et al.*, Phys. Rev. Lett. **89**, 040402 (2002).
[7] M. Greiner, O. Mandel, T.W. Hänsch, and I. Bloch, Nature (London) **415**, 39 (2002); M. Greiner *et al.*, *ibid.* **419**, 51 (2002).
[8] O. Mandel *et al.*, Phys. Rev. Lett. **91**, 010407 (2003).
[9] E. L. Bolda, E. Tiesinga, and P. S. Julienne, Phys. Rev. A **66**, 013403 (2002). For an optical Feshbach resonance, see M. Theis *et al.*, Phys. Rev. Lett. **93**, 123001 (2004).
[10] See, for example, S. Sachdev, *Quantum Phase Transitions* (Cambridge University, Cambridge, England, 1999).
[11] G. Vidal, Phys. Rev. Lett. **91**, 147902 (2003).
[12] M. Rigol and A. Muramatsu, cond-mat/0403387.
[13] D. Petrov, cond-mat/0404036.
[14] G. Nogues *et al.*, Nature (London) **400**, 239 (1999).
[15] L. S. Levitov, in *Quantum Noise in Mesoscopic Physics*, edited by Y. V. Nazarov (Kluwer Academic, Dordrecht, 2002).
[16] See, for example, M. A. Cazalilla and J. B. Marston, Phys. Rev. Lett. **88**, 256403 (2002).